Generation of Integration-Free Porcine Induced Neural Stem Cells Using Sendai virus

Warunya Chakritbudsabong
Mahidol University Faculty of Veterinary Science
Ruttachuk Rungsiwiwut
Srinakharinwirot University Faculty of Medicine
Ladawan Sariya
Mahidol University Faculty of Veterinary Science
Phakhin Juntahirun
Mahidol University Faculty of Veterinary Science
Nattarun Chaisilp
Mahidol University Faculty of Veterinary Science
Somjit Chaiwattanarungruengpaisan
Mahidol University Faculty of Veterinary Science
Sasitorn Rungarunlert (sasitorn.run@mahidol.edu)
Mahidol University, Faculty of Veterinary Science https://orcid.org/0000-0001-5500-1295

Research

Keywords: Sendai virus, induced neural stem cells, reprogramming, porcine, self-renewal, neuron, astrocyte, differentiation

Posted Date: October 1st, 2021

DOI: https://doi.org/10.21203/rs.3.rs-948414/v1

Generation of Integration-Free Porcine Induced Neural Stem Cells Using Sendai virus

Warunya Chakritbudsabong[1,2], Ruttachuk Rungsiwiwut[3], Ladawan Sariya[4], Phakhin Juntahirun[1,2], Nattarun Chaisilp[4], Somjit Chaiwattanarungruengpaisan[4], Sasitorn Rungarunlert[1,2*]

[1] Laboratory of Cellular Biomedicine and Veterinary Medicine, Faculty of Veterinary Science, Mahidol University, Nakhon Pathom 73170, Thailand

[2] Department of Preclinic and Applied Animal Science, Faculty of Veterinary Science, Mahidol University, Nakhon Pathom 73170, Thailand

[3]Department of Anatomy, Faculty of Medicine, Srinakharinwirot University, Bangkok, Thailand.

[4]The Monitoring and Surveillance Center for Zoonotic Disease in Wildlife and Exotic Animals (MOZWE), Faculty of Veterinary Science, Mahidol University, Nakhon Pathom 73170, Thailand

*Correspondence: sasitorn.run@mahidol.edu

*** Correspondence:**

Sasitorn Rungarunlert

sasitorn.run@mahidol.edu

Abstract

Background

The reprogramming of cells to induced neural stem cells (iNSCs), faster and safer to generate than induced pluripotent stem cells, holds tremendous promise for disease modeling and personalized cell-based therapies for neurological diseases. Porcine iNSCs (piNSCs) may serve as a disease model for human medicine, as pigs are one of the most successful large animal models in

biomedical research. Thus, this study aimed to establish safe and efficient integration-free piNSC lines.

Methods

The integration-free piNSC lines were generated by reprogramming porcine fibroblasts using the Sendai virus (SeV).

Results

Here we report the successful generation of integration-free piNSC lines using the SeV, with a reprogramming efficiency of 0.4%. The piNSCs can be expanded for up to 40 passages and express high levels of NSC markers (PAX6, NESTIN, and SOX2). They can produce neurons and glia, expressing TUJ, MAP2, TH, and GFAP. No induced pluripotent stem cells developed during reprogramming, and the established piNSCs did not express OCT4. Hence, the SeV can reprogram porcine fibroblast without first going through an intermediate pluripotent stage.

Conclusions

With the SeV approach, we generated integration-free piNSCs that may be used to assess the efficacy and safety of iNSC-based clinical translation in humans.

Keywords: Sendai virus, induced neural stem cells, reprogramming, porcine, self-renewal, neuron, astrocyte, differentiation

1. Introduction

The remarkable discovery that differentiated cells are able to be completely reprogrammed to induced pluripotent stem cells (iPSCs) by viral-mediated transduction of exogenous transcription factors marks a significant breakthrough in regenerative medicine [1]. The iPSCs offer an infinite supply of differentiated cells for various purposes, including disease modeling *in vitro*, drug

research, toxicity testing, and autologous cell-based therapy [2]. The potential for patient-specific cells to be used in autologous cell-based treatments is quite intriguing. The generation of neural stem cells (NSCs) and neurons from iPSCs is one of the most clinically relevant cell types [3-5]. Nevertheless, this process is complicated by several factors, including the lengthy and inefficient reprogramming and differentiation process [6], heterogenous cell differentiation [7], the possibility of tumor development as a result of undifferentiated iPSCs surviving in the differentiated iPSC population [4], and genomic instability [8].

Alternatively, the forced expression of the NSC transcription factors [9-11] or the pluripotency transcription factors, encoding Oct3/4, Sox2, Klf4, and c-Myc (OSKM) [12-14] converts differentiated cells directly into induced neural stem cells (iNSCs) and induced neural progenitor cells (iNPCs). This approach is an appealing alternative to existing iPSC technology because it enables the production of patient-specific NSCs without passing through the pluripotent stage, thereby decreasing the risk of tumorigenic potential [15, 16]. Since the first mouse iNSCs (miNSCs) were established in 2011 [12], many studies have been published detailing the derivation of iNSCs from a variety of species, including rats [17], monkeys [18] and humans [18-20]. The established iNSCs have numerous features in common with embryonic brain-derived NSCs, such as morphological, self-renewal capacity, gene and protein expression profiles, epigenetic state, as well as functional multipotency *in vitro* and *in vivo* [9, 21, 22]. Additionally, when iNSCs are transplanted into animal models for up to 6 months, they can alleviate disease phenotypes without developing tumors, demonstrating their therapeutic promise for neurological disorders [23].

Although the iNSCs have been discovered as a feasible, effective, and autologous source for medical applications, their therapeutic potential has yet to be fully explored. Porcine iNSCs (piNSCs) may serve as a disease model for human regenerative medicine, as pigs have established themselves as one of the most effective large animal models in biomedical research, often regarded as a preferable alternative to rodent models [24-26]. Furthermore, preclinical evaluation of stem cell transplantation using piNSCs and their differentiation cells may be utilized to determine the safety and efficacy of iNSCs prior to human trials. Importantly, piNSCs are also an appealing cell source for investigating pig disease in veterinary medicine. However, no commercially available piNSC and their neural differentiation exist for studying pig neurological diseases, such as *Streptococcus suis* infections and African Swine Fever. Until now, only one group has reported success in generating piNPCs using nonintegrating episomal plasmids. They demonstrated that piNPCs retain the capacity to grow for an extended period of time and differentiate efficiently into neurons *in vitro* [27].

Although previous studies have established a number of methods for directly converting somatic cells to iNSCs, most of the investigations rely on integrating viral vectors (such as lentiviral or retroviral approaches) [9, 13, 15, 28, 29]. These methods may result in insertional mutagenesis and the persistence or reactivation of transgenes. Moreover, therapeutic translation of this technique will require a thorough safety evaluation of any mutations gained during the reprogramming process, as well as a fast derivation and differentiation strategy [30]. A Sendai virus (SeV) vector can overcome these issues owing to a single-stranded RNA virus propagating in the cytoplasm of infected cells that does neither pass a DNA phase nor integrate into the host genome, unlike the other viruses. As a result, the risks of tumorigenesis can be reduced throughout the reprogramming

process [31]. With the SeV delivery system in kits, researchers may easily transduce the desired cells with SeV carrying OSKM for reprogramming and quickly remove SeV and transgenes by temperature change as temperature-sensitive. Recently, SeV-based vectors have been widely utilized to generate human, and mouse integration-free iPSCs [32-35] and have been adapted to generate iNSCs from human and monkey postnatal and adult fibroblasts [18]. However, the generation of piNSCs using the Sev has not been explored yet.

To extend our findings into clinical applications, therapeutic approaches will rely mainly on personalized iNSC transplantation. We emphasize here that iNSCs require an effective cryopreservation method in order to obtain good results upon transplantation. Cryopreservation enables the storage and transportation of iNSCs for clinical purposes. Thus, iNSCs should be cryopreserved with a high survival rate and minimal influence on cellular characteristics like proliferation and differentiation potential during freezing and thawing. Ascorbic acid (Vitamin C) is a water-soluble antioxidant that neutralizes the oxidative effects of radicals from the cryopreservation process. To improve the survival of iNSCs during the cryopreservation procedure, ascorbic acid was pretreated at various concentrations before freezing and its neuroprotective effects were evaluated.

In this investigation, we generated integration-free piNSC lines from pig fibroblasts by utilizing a Sendai virus approach. The piNSCs displayed typical features of NSCs such as morphology, gene expression patterns, self-renewal capacity, and differentiation potential. Moreover, pretreatment of iNSCs with ascorbic acid did not affect the viability of iNSCs during the cryopreservation procedure. We anticipate that piNSCs will serve as novel, easily accessible large animal models

for evaluating the efficacy and safety of iNSC-based clinical translation. This pig model will allow us to assess the ultimate feasibility of cell-based regenerative therapy. Furthermore, our integration-free piNSCs might be useful for disease modeling in pigs. As a result, this discovery is beneficial for both veterinary medicine and the possibility of translation to human medicine.

2. Materials and Methods

2.1 Ethics Statement

The Institutional Animal Care and Use Committee at the Faculty of Veterinary Science, Mahidol University, Thailand, reviewed and approved the experimental animal used in this study (Approval ID: MUVS-2015-49). The Mahidol University Biosafety Subcommittee approved the use of all biohazardous items in this work, including animal cells and recombinant DNA (MU-2013-002).

2.2 Cell Culture

All chemical compounds and cell culture reagents were acquired from Sigma-Aldrich (St. Louis, MO, USA) or Thermo Fisher Scientific (Waltham, MA, USA), unless otherwise specified. All cells were incubated in a humidified 5% CO_2 incubator at 37°C.

2.3 Generation of piNSCs

A porcine tail was received from an authorized farm in Ratchaburi Province, Thailand. Porcine tail fibroblasts (PTFs) were extracted using standard procedures from the tail of a three-day-old crossbred piglet, with minor modifications [36]. The PTFs were propagated in fibroblast medium (FM) containing DMEM-high glucose, 10% fetal bovine serum (cat. no. SV30160, Hyclone, Logan, UT, USA), 1% Antibiotic-Antimycotic solution, and 1% GlutaMAX™. All cells were

grown on feeder-free culture system (Matrigel-coated dishes or plates) throughout the piNSC generation process. The PTFs were reprogrammed utilizing the integration-free CytoTune™-iPS 2.0 Sendai reprogramming kit incorporating human reprogramming factors, OSKM in FM following the manufacturer's instruction, with modifications (**Fig. 1A**). The PTFs (passages 3) were seeded on 6-well plates at a density of $1x10^4$ cells/cm^2 one day before viral transduction to achieve approximately 60–70% confluency at the time of transduction. The PTFs were transfected with SeV at a multiplicity of infection (MOI) of 5 in a FM for 24 h. The next day, the culture medium containing the Sendai virus was removed and renewed with a FM. The following day, the medium was switched to the iNSC medium (iNSCM) comprising DMEM/F-12 and Neurobasal medium in a ratio of 1:1 supplemented with 2% B-27™ Supplement, 1% N-2 Supplement, 1% antibiotic-antimycotic solution, 1% GlutaMAX™, 20 ng/mL human basic fibroblast growth factor (bFGF; R&D Systems), and 10 ng/mL human epidermal growth factor (hEGF). Seven days after reprogramming, the cells were dissociated with a 0.25% trypsin-EDTA solution and replaced onto Matrigel-coated plate in piNSCM. From then on, the appearance of epithelium-like colonies was monitored, and the medium was changed daily. Colonies with epithelium-like morphology were large enough to be picked up around days 16 to 21 and transferred onto an IVF one-well dish for expansion. Every 2–3 days, sub-culturing at a 1:5 ratio with Versene® Solution was conducted consistently for further experiments.

2.4 The piNSC Freezing and Thawing

The piNSCs were passaged and plated at a density of $3x10^5$ cells per well in 6-well plates, then treated with ascorbic acid at various doses (0, 10, 50, and 100 uM) into NSC cultured medium for 12 hours before freezing to test the protective effects of ascorbic acid on cryopreservation of

piNSCs. A total of 5 × 10^5 cells was dissociated and placed in a cryo-tube (Nunc CryoTubes, Thermo Fisher Scientific Inc., MA, USA) with 1 ml cryopreservation solution (iNSC medium with 10% DMSO). The vials were placed in a freezing container (Nalgene Mr. Frosty, Thermo Fisher Scientific, MA, USA) for 24 h in a -80C freezer for cryopreservation. Subsequently, the vials were transferred to LN_2 and stored for 1 week before thawing.

2.5 Cell Proliferation and Measurement of Nitrite Production

After thawing, the cells were plated at a density of 1x10^4 cells per well in a 96-well plate and maintained for 2 days in an iNSC medium. The cell proliferation was assessed using the Cell Counting Kit-8 (CCK-8) assay, and the levels of nitric oxide (NO) were measured using the Griess reagent (Promega) at various time points after thawing (at 1, 6, 12, 24, 36, and 48 h). A cell proliferation study was performed by adding 10 ul of the CCK-8 reagent to live cells in 96-well plates, and the suspension NSCs (100 ul/well) were incubated for 3 hours at 37°C with 5% CO_2 to determine cell proliferation. The absorbance at 450 nm was used to determine the vitality of cells. For Griess analysis, supernatant from each well was collected and transferred to a new tube. Following centrifugation, 100 L of the supernatant was transferred to a new 96-well plate and diluted with equivalent volumes of Griess reagent. For 10 min at 37°C, the plate was incubated in the dark. The absorbance of the reaction product was evaluated at 550 nm using a microplate reader (Bio-Rad, CA, USA). The amount of nitrite in control and treated cells was determined using a sodium nitrite standard reference curve and represented as μM nitrite/mL [37].

2.6 Neurosphere Formation

The formation of neurospheres was investigated for iNSCs by resuspending 10,000 cells per well in iNSCM in 96-well plates covered with poly (2-hydroxyethyl methacrylate). Every two days, a fresh medium is added to the suspension cultures. Neurospheres were counted using a light microscope seven days after the suspension and collected for further study.

2.7 Differentiation of piNSCs

To induce spontaneous neuronal differentiation, piNSCs (P20) were dissociated and re-plated into a 6 well dish or a 24 well plate with matrigel-coated at a density of 2 x 10^4 cells per cm^2 in the neuronal differentiation medium (the piNSCM without bFGF and hEGF). The media was replaced every two days for 14 days. Phase-contrast image analysis was performed every day to monitor cell differentiation in each well. At days 0 (proliferating piNSCs) and 14 (neuronal differentiation), the cells were fixed with 4% paraformaldehyde for immunofluorescence analysis and were manually detached for western blot analysis.

2.8 G-banding Karyotype Analysis

The karyotype analysis followed a previously described procedure with minor modifications [38]. Briefly, piNSC lines (P20) were cultured in a 6 cm culture dish at approximately 70% confluence and treated with a 5 μg/mL colcemid solution (KaryoMAX™ Solution) for 1 h at 37°C. The cells were gently dissociated using Versene® Solution and then treated for 15 min at 37°C with a hypotonic solution (75 M KCL). They were treated in a cold fixing solution (1:3 acetic acid to methanol concentration) 3 times. The fixed cells were transferred to cool microscope slides and maintained at 37°C overnight. After soaking the slides in 0.05 percent trypsin EDTA solution at 37°C, they were stained with Giemsa solution. The images of 50 G-banded metaphases were

captured by a Nikon Eclipse Ni with DS-Ri2 Camera (Nikon Instruments, Japan) and analyzed by LUCIA Cytogenetics (Nikon Instruments, Japan).

2.9 Immunofluorescence and imaging analysis

The immunofluorescence analysis was utilized to detect NSC markers and distinguish neuronal cell lineages. Samples were fixed with 4% paraformaldehyde in cold phosphate-buffered saline (PBS) at 37°C for 15 min. Then, samples were permeabilized with 0.25% Triton-X 100 in PBS at 37°C for 10 min and incubated with a non-specific binding blocking solution (2% bovine serum albumin in PBS) at 37°C for 1 h. Samples were treated overnight at 4°C in the dark with primary antibodies and then for 1 hour at 37°C with secondary antibodies, as shown in Table 1. The coverslips were mounted on glass slides with antifade mounting medium with DAPI (Vectashield, Vector Laboratories, Burlingame, CA), and visualized using a Leica DMi8 inverted fluorescence microscope equipped with a Leica DFC7000 camera and the TCS SP8 confocal microscope equipped with a DFC3000G camera (Leica Microsystems, Wetzlar, Germany). For each sample, at least 40 z-stacks with 0.6-0.7 m intervals were acquired. All images were analyzed using the Leica Application Suite X (LAS X) imaging or ImageJ (NIH, USA) software to detect single fluorescence intensity measurements, the number of fluorescence positive cells and co-localization. The images were measured in 20 randomly selected fields on each slide at a magnification of ×200. At least three slides were scanned for each group to determine the expression of these markers (n = 3 independent experiments). Data is presented as the mean fluorescence intensity value ± SEM after background signal subtraction. The percentage of positive cells per total number is based on the number of fluorescence marker-positive cells and DAPI-positive cell numbers measured by DAPI nuclear staining using ImageJ.

2.10 SeV genome and transgenes analysis

The expression of the SeV genome and transgenes in both piNSCs was determined using RT-PCR. Cells were lysed and RNA extracted using the RNeasy Mini Kit (Genaid Biotech Ltd., New Taipei City, Taiwan). The SuperScript™ III First-Strand Synthesis System was then used to reverse transcribe 1 g of total RNA to cDNA. 50 ng template cDNA, 12.5L GoTaq PCR master mix (Promega, WI, USA), and 0.2M of each primer were used in the PCR reaction. The PCR-amplified separation was achieved on 2% agarose gels and imaged using GelRed® nucleic acid staining (Biotium, Fremont, CA, USA).

2.11 Western Blot Analysis

The cells were lysed using sonication in a radioimmunoprecipitation assay buffer, and the total protein concentration was examined by a protein assay kit (Bio-Rad Laboratory, Hercules, CA, USA). Western blot analysis was determined to identify interesting proteins in 25 capillary cartridges according to the 12–230 kDa Jess & Wes Separation Module protocol (SM-W004, ProteinSimple, San Jose, CA, USA). Table 1 lists the primary antibodies. The results were analyzed using Compass for Simple Western version 5.0.1 software (Build 0911; ProteinSimple).

2.12 Statistical Analysis

Each experiment was conducted a minimum of three times. The quantitative results were expressed as the mean ± standard error of the mean (SEM). The data was analyzed statistically using one-way analysis of variance (ANOVA) for comparisons of more than two groups and the Student's t-test for comparisons of two groups. Additionally, Tukey's test was employed as a post hoc multiple

comparison test for differences. All statistical analyses were carried out using the SPSS version 25 software (IBM, USA). Statistical significance was defined as $p < 0.05$.

3. Results

3.1 Transgene-Free piNSC lines Are Generated from PTFs using the Sendai Virus

To address the question of whether PTFs can be directly converted into stably expanding multipotent piNSCs, PTFs were isolated from the tail of a three-day-old crossbred piglet (Large White/Landrace × Duroc). Non-integrative Sendai viral vectors carrying OSKM were transfected into PTFs for 24 h (**Fig. 1B**). After that, cells were cultured in FM for one day to recovery and then in iNSCM for another day. On day 7 after transduction, the cells were dissociated and transferred onto Matrigel-coated 6 well plates in piNSCM at a density of 1 x 10^4 cells per well. On day 11 after transduction, the iNSC clusters with neuroepithelial-like morphology emerged and developed quickly over the next week. On days 16-21, the neuroepithelial-like morphology colonies were mechanically triturated into small clusters, and re-plated onto Matrigel-coated coverslips for immunostaining or onto a Matrigel-coated one-well dish for cell expansion in iNSCM (**Fig. 1C, 1D**). The neuroepithelial colonies expressing early NSC markers such as PAX6, NESTIN, and SOX2 were continuously propagated using TrypLE Select Enzyme along the serial passaging for further characterization (**Fig. 1E-1G**). Hence, the transfection efficiency was 0.40%, as measured by the number of neuroepithelial colonies expressing PAX6, NESTIN, and SOX2 divided by the total number of transfected cells. We generated a total of nine iNSC lines capable of proliferation in adherent monolayers (2D) (**Fig. 1H**) or neurospheres (3D) (**Fig. 1I**) as suspension-grown neural cell aggregates and differentiation into neural lineages (**Fig. 1J**). We chose only two iNSC lines based on their indefinite self-renewal potential and multipotency

differentiation, namely VSMUi002-B and VSMUi002-E, for further analysis. To remove the temperature-sensitive SeV vectors, iNSCs were cultured at 39 °C in an incubator for 4 weeks, after which the cells were collected every week for PCR detection of the remaining virus. The SeV vectors were positive at passage 9 but vanished at passage 12, indicating that SeV vectors had been completely eradicated.

3.2 Transgene-Free piNSC Lines Exhibit Characteristics of NSCs

At passage 20, both piNSC lines (VSMUi002-B and VSMUi002-E) displayed a neuroepithelial morphology in adherent monolayers (**Fig. 2A**). They displayed a high percentage of cells expressing the NSC markers, with nearly 100% of cells staining positive for PAX6, SOX2, and NESTIN, as determined by quantitative immunofluorescence analysis, indicating the formation of a highly homogeneous population (**Fig. 2A, 2B**). However, they did not express pluripotency-related genes, OCT4 (**Fig. 2A**). As a result, the absence of OCT4 established that piNSC lines did not originate from intermediate pluripotent stages. To corroborate the immunofluorescence results, the endogenous PAX6 and SOX2 proteins in piNSCs were quantified by western blot analysis in comparison to their parental PFFs. The expression of PAX6 and SOX2 was substantially higher in VSMUi002-E than in VSMUi002-B. The PTF lacked both PAX6 and SOX2 protein expression (**Fig. 2C**). The piNSC lines (VSMUi002-B and VSMUi002-E) had a high percentage of cells expressing the proliferation marker Ki67 (75.3% ± 1.18% and 78.6% ± 1.19%, respectively) (**Fig. 2A, 2B**). Furthermore, the population cell doubling time of the VSMUi002-B and VSMUi002-E cell lines was approximately 24 h, with no significant difference ($P > 0.05$), and the cells had been passaged over 40 times. Hence, both iNSC lines had a strong capacity for self-renewal. They exhibited a typical diploid porcine karyotype (38, XY) during long term culture (**Fig. 2D**). Both

piNSC lines were able to form neurospheres (3D) in suspension cultures with similar efficiency, which were homogeneous in size and shape on day 7 (**Fig. 3A, 3B**). Additionally, immunofluorescence labeling revealed that the neurospheres expressed NSC markers (PAX6 and SOX2) and a proliferation marker (Ki67) (**Fig. 3A**). Thus, piNSCs display neural progenitor features that can be obtained from PTF by Sendai virus reprogramming.

3.3 The piNSCs Spontaneously Differentiate to Neurons and Glia

To determine the ability of piNSCs to differentiate spontaneously, they were dissociated into single cells and grown on a Matrigel substrate in a neural differentiation medium. After 7 days of differentiation, piNSCs revealed significant morphological alterations, including a decrease in cell body size (**Fig. 4A**), and expressed the immature neuronal marker (TUJ1). At day 14, the piNSCs exhibited mature neuronal morphology, including extensive and complex neurites, which were positive for the mature neuronal marker (MAP2) (**Fig. 4A, 4B**). The merged immunofluorescence images revealed a co-localization of TUJ and MAP. Consistent with these findings, high levels of MAP2 protein expression colocalized with TUJ1 staining in VSMUi002-B and VSMUi002-E, with Pearson's correlation of 0.61 ± 0.02 and 0.79 ± 0.01, respectively. Additionally, some TUJ1-positive neurons were labeled with the synaptic protein synaptophysin (SYP) along neurites in a punctate manner (**Fig. 4B**), indicating possible synaptic connections. Furthermore, piNSCs have a high capacity for differentiation into dopamine-secreting neurons expressing tyrosine hydroxylase (TH) (**Fig. 4B**). The piNSCs also developed into glial fibrillary acidic protein (GFAP)-positive astrocytes (**Fig. 4B**). The staining intensities of all neuronal-positive cells (TUJ1, MAP, TH, SYN, and GFAP) are the same in both iNSC lines (**Fig. 4C**). Moreover, qPCR analysis indicated an increase in the expression of myelin basic protein (MBP), which is expressed mostly in

oligodendrocytes (**Fig. 4D**), indicating the existence of oligodendrocytes in the differentiated derivatives. To corroborate the immunofluorescence results, the endogenous TUJ1, MAP2 and GFAP proteins in iNSC-derived neural differentiation were quantified by western blot analysis in comparison to their parental iNSCs. The expressions of those proteins were substantially higher in the neuronal differentiated from VSMUi002-E than in those from VSMUi002-B (**Fig. 4B**). Both iNSCs lacked both MAP2 and GFAP protein expression (**Fig. 4B**). Interestingly, VSMUi002-E also expressed TUJ1 during NSC stage. Taken together, our data indicate that piNSCs have the capacity for multipotent neuronal differentiation.

3.4 Ascorbic acid had no neuroprotective impact on cryopreservation of piNSCs.

The piNSCs were treated with ascorbic acid at 0, 10, 50, and 100 uM for 24 h before freezing to investigate the protective effects of ascorbic acid on cryopreservation. The cells were cultured in 24 well plates after being thawed for 24 hours and stained with KI67 for cell proliferation and CASPASE 3 for cell apoptosis. Our findings revealed no significant differences in KI67 positive cells across different concentrations of ascorbic acid (**Fig. 5A, 5B**). Furthermore, the absence of CASPASE 3 positivity after freezing suggested that the cells did not undergo apoptosis. Furthermore, after freezing, the cells were analyzed for cell proliferation using the CCK-8 test and for nitric oxide (NO) levels using the Griess assay at 1, 6, 12, 24, 36, and 48 h. Our results indicated that piNSCs grown in the absence of ascorbic acid proliferated more rapidly than those grown in the presence of other ascorbic acid concentrations at 48 h (**Fig. 5C**). No significant differences in NO levels across different concentrations of ascorbic acid (**Fig. 5D**). Our results revealed that ascorbic acid had no neuroprotective impact on the cryopreservation of piNSCs.

4. Discussion

Here, we describe a safety approach for reprogramming porcine fibroblasts into iNSCs using the temperature-sensitive SeV that has several benefits over prior studies: (i) the use of non-integration SeV approaches avoids vector and transgenic sequences from being integrated into the iNSC genome. While, retrovirus- or lentivirus-based integration approaches may result in interruption of endogenous gene expression as well as the possibility of transgene reactivation [18, 26]; (ii) our piNSCs exhibit self-renewal and multipotency into neuronal and glial lineages without going through pluripotent state, making them a safer alternative to piPSCs; (iii) stable, self-renewing iNSCs can be generated from pig sources, which is advantageous for determining the safety and efficacy of iNSCs prior to human trials and an attractive cell source for studying pig disease in veterinary medicine [27].

Integrating techniques are frequently based on viral vector systems, which have been widely utilized and verified for the production of transgenic animal models and cell lines. Retroviral and lentiviral vectors incorporate into the target genome, causing lasting genetic changes to the host genome and frequently affecting the transcriptome through persistent transgene expression [9, 13, 15, 28]. Thus, while numerous studies have effectively transdifferentiated somatic cells into iNSCs using retro- or lentiviral vectors, a transgenic factor-free procedure would be desirable to minimize the possibility of irreversible genetic alterations impairing the normal function of the generated iNSCs. Alternatively, non-integrating methods for generating transgene-free iNSCs have been devised, including the use of episomal vectors and the Sendai virus in combination with or without small molecules [39-41]. The use of episomal vector is very inexpensive and easily adaptable to reprogramming a variety of cell types, both iPSCs and iNSCs. Episomal vectors are eliminated

from these iPSCs by several passages through cell divisions, which can take several months to achieve transgene-free iPSCs [30, 42]. However, Xu and colleagues indicated that ipNPCs contained virtually undetectable amounts of EBNA-1, but episomal vector-transfected PFFs carried approximately 100 copies per cell, suggesting that EBNA-1 was not present in the ipNPC genome [27].

An alternative method, SeV, was used to generate iNSCs as a non-integrating viral vector [18]. SeV is a negative-sense single-stranded RNA virus that infects predominantly mammalian cells and replicates solely in their cytoplasm. SeV-based vectors have increasingly been utilized to generate transgene-free iPSCs in recent years and have been modified to generate iNSCs from human and monkey postnatal and adult fibroblasts [18, 43]. Additionally, we succeeded in generating integration-free piNSC lines with a reprogramming efficiency of 0.4% utilizing the SeV. Similar to previous research, the established piNSCs exhibited NSC markers (PAX6, SOX2, and NESTIN) and demonstrated self-renewal potential as determined by immunocytochemical labeling for proliferation markers such as Ki-67 in conjunction with essential markers for NSCs [18, 27, 43]. Furthermore, the SeV method did not generate iPSCs, and the lack of OCT4 demonstrated that piNSC lines did not come from intermediate pluripotent phases. As a result, piNSCs are safer than piPSCs [15, 16]. Hence, the SeV provides an alternative integration-free reprogramming method that removes the danger of genetic alterations and enhances the prospects of iNSCs from bench to bedside. As with previous research, the established piNSCs are multipotent stem cells capable of generating neurons and glial cells [44]. However, differentiation capacity varies according to the iNSC population and the differentiation technique utilized in vitro (e.g., spontaneous, undirected, and directed in vitro differentiation approaches). Our findings

confirmed that these piNSCs pretend to be differentiated into neurons and astroglia since development into oligodendrocytes was less effective due to the short differentiation phase, consistent with previous research [45].

Moreover, we demonstrated that ascorbic acid has no neuroprotective effect on piNSC cryopreservation. Contrary to another study, the NSCs generated in this culture system supplement with ascorbic acid preserved their long-term growth capability, neural pluripotency, and ability to differentiate into functional neurons [46].

5. Conclusions

Using the SeV for reprogramming, we effectively produced integration-free piNSC lines without going through an intermediate pluripotent stage. To our information, this is the first attempt to use the SeV to direct the reprogramming of somatic cells into NSC in a porcine species. As a potential model species, piNSCs may provide an intriguing tool for determining the ultimate feasibility of cell-based regenerative treatment for human medicine and disease modeling in pigs. As a result, this finding is useful for veterinary medicine and the prospect of human medical translation.

6. Availability of data and materials

This published paper contains all data produced and/or analyzed during this investigation.

7. Abbreviations

iNSCs: induced neural stem cells

piNSCs: porcine induced neural stem cells

SeV: Sendai virus

NSCs: neural stem cells

OSKM: Oct3/4, Sox2, Klf4, and c-Myc

miNSCs: mouse induced neural stem cells

PTFs: Porcine tail fibroblasts

FM: fibroblast medium

MOI: multiplicity of infection

iNSCM: iNSC medium

bFGF: basic fibroblast growth factor

hEGF: human epidermal growth factor

CCK-8: Cell Counting Kit-8

NO: nitric oxide

PBS: phosphate-buffered saline

8. Reference

1. Takahashi K, Yamanaka S. Induction of pluripotent stem cells from mouse embryonic and adult fibroblast cultures by defined factors. Cell. 2006;126(4):663-76. doi: 10.1016/j.cell.2006.07.024.
2. Moradi S, Mahdizadeh H, Saric T, Kim J, Harati J, Shahsavarani H, et al. Research and therapy with induced pluripotent stem cells (iPSCs): social, legal, and ethical considerations. Stem Cell Res Ther. 2019;10(1):341. doi: 10.1186/s13287-019-1455-y.
3. Du ZW, Chen H, Liu H, Lu J, Qian K, Huang CL, et al. Generation and expansion of highly pure motor neuron progenitors from human pluripotent stem cells. Nat Commun. 2015;6:6626. doi: 10.1038/ncomms7626.
4. Lopez-Serrano C, Torres-Espin A, Hernandez J, Alvarez-Palomo AB, Requena J, Gasull X, et al. Effects of the Post-Spinal Cord Injury Microenvironment on the Differentiation Capacity of Human Neural Stem Cells Derived from Induced Pluripotent Stem Cells. Cell Transplant. 2016;25(10):1833-52. doi: 10.3727/ 096368 916X691312.

5. Lu J, Zhong X, Liu H, Hao L, Huang CT, Sherafat MA, et al. Generation of serotonin neurons from human pluripotent stem cells. Nat Biotechnol. 2016;34(1):89-94. doi: 10.1038/nbt.3435.
6. Hu BY, Weick JP, Yu J, Ma LX, Zhang XQ, Thomson JA, et al. Neural differentiation of human induced pluripotent stem cells follows developmental principles but with variable potency. Proc Natl Acad Sci U S A. 2010;107(9):4335-40. doi: 10.1073/pnas.0910012107.
7. Chambers SM, Fasano CA, Papapetrou EP, Tomishima M, Sadelain M, Studer L. Highly efficient neural conversion of human ES and iPS cells by dual inhibition of SMAD signaling. Nat Biotechnol. 2009;27(3):275-80. doi: 10.1038/nbt.1529.
8. Weissbein U, Ben-David U, Benvenisty N. Virtual karyotyping reveals greater chromosomal stability in neural cells derived by transdifferentiation than those from stem cells. Cell Stem Cell. 2014;15(6):687-91. doi: 10.1016/j.stem.2014.10.018.
9. Han DW, Tapia N, Hermann A, Hemmer K, Hoing S, Arauzo-Bravo MJ, et al. Direct reprogramming of fibroblasts into neural stem cells by defined factors. Cell Stem Cell. 2012;10(4):465-72. doi: 10.1016/j.stem.2012.02.021.
10. Sheng C, Zheng Q, Wu J, Xu Z, Wang L, Li W, et al. Direct reprogramming of Sertoli cells into multipotent neural stem cells by defined factors. Cell Res. 2012;22(1):208-18. doi: 10.1038/cr.2011.175.
11. Lujan E, Chanda S, Ahlenius H, Sudhof TC, Wernig M. Direct conversion of mouse fibroblasts to self-renewing, tripotent neural precursor cells. Proc Natl Acad Sci U S A. 2012;109(7):2527-32. doi: 10.1073/pnas.1121003109.
12. Kim J, Efe JA, Zhu S, Talantova M, Yuan X, Wang S, et al. Direct reprogramming of mouse fibroblasts to neural progenitors. Proc Natl Acad Sci U S A. 2011;108(19): 7838-43. doi: 10.1073/pnas.1103113108.
13. Thier M, Worsdorfer P, Lakes YB, Gorris R, Herms S, Opitz T, et al. Direct conversion of fibroblasts into stably expandable neural stem cells. Cell Stem Cell. 2012;10(4):473-9. doi: 10.1016/j.stem.2012.03.003.
14. Cairns DM, Chwalek K, Moore YE, Kelley MR, Abbott RD, Moss S, et al. Expandable and Rapidly Differentiating Human Induced Neural Stem Cell Lines for Multiple

Tissue Engineering Applications. Stem Cell Reports. 2016;7(3):557-70. doi: 10.1016/j.stemcr.2016.07.017.

15. Ring KL, Tong LM, Balestra ME, Javier R, Andrews-Zwilling Y, Li G, et al. Direct reprogramming of mouse and human fibroblasts into multipotent neural stem cells with a single factor. Cell Stem Cell. 2012;11(1):100-9. doi: 10.1016/j.stem.2012.05. 018.
16. Gao M, Yao H, Dong Q, Zhang H, Yang Z, Yang Y, et al. Tumourigenicity and Immunogenicity of Induced Neural Stem Cell Grafts Versus Induced Pluripotent Stem Cell Grafts in Syngeneic Mouse Brain. Sci Rep. 2016;6:29955. doi: 10.1038/srep 29955.
17. Xi G, Hu P, Qu C, Qiu S, Tong C, Ying QL. Induced neural stem cells generated from rat fibroblasts. Genomics Proteomics Bioinformatics. 2013;11(5):312-9. doi: 10.1016 /j.gpb.2013.09.003.
18. Lu J, Liu H, Huang CT, Chen H, Du Z, Liu Y, et al. Generation of integration-free and region-specific neural progenitors from primate fibroblasts. Cell Rep. 2013;3(5):1580-91. doi: 10.1016/j.celrep.2013.04.004.
19. Wang L, Wang L, Huang W, Su H, Xue Y, Su Z, et al. Generation of integration-free neural progenitor cells from cells in human urine. Nat Methods. 2013;10(1):84-9. doi: 10.1038/nmeth.2283.
20. Kwak TH, Hali S, Kim S, Kim J, La H, Kim KP, et al. Robust and Reproducible Generation of Induced Neural Stem Cells from Human Somatic Cells by Defined Factors. Int J Stem Cells. 2020;13(1):80-92. doi: 10.15283/ijsc19097.
21. Kim SM, Flasskamp H, Hermann A, Arauzo-Bravo MJ, Lee SC, Lee SH, et al. Direct conversion of mouse fibroblasts into induced neural stem cells. Nat Protoc. 2014;9(4):871-81. doi: 10.1038/nprot.2014.056.
22. Yao H, Gao M, Ma J, Zhang M, Li S, Wu B, et al. Transdifferentiation-Induced Neural Stem Cells Promote Recovery of Middle Cerebral Artery Stroke Rats. PLoS One. 2015;10(9):e0137211. doi: 10.1371/journal.pone.0137211.
23. Hemmer K, Zhang M, van Wullen T, Sakalem M, Tapia N, Baumuratov A, et al. Induced neural stem cells achieve long-term survival and functional integration in the adult mouse brain. Stem Cell Reports. 2014;3(3):423-31.doi: 10.1016/j.stemcr.2014. 06.017.

24. Harding J, Roberts RM, Mirochnitchenko O. Large animal models for stem cell therapy. Stem Cell Res Ther. 2013;4(2):23.
25. Xu J, Yu L, Guo J, Xiang J, Zheng Z, Gao D, et al. Generation of pig induced pluripotent stem cells using an extended pluripotent stem cell culture system. Stem Cell Res Ther. 2019;10(1):193. doi: 10.1186/s13287-019-1303-0.
26. Chakritbudsabong W, Chaiwattanarungruengpaisan S, Sariya L, Pamonsupornvichit S, Ferreira JN, Sukho P, et al. Exogenous LIN28 Is Required for the Maintenance of Self-Renewal and Pluripotency in Presumptive Porcine-Induced Pluripotent Stem Cells. Front Cell Dev Biol. 2021;9:709286.
27. Xu XL, Yang JP, Fu LN, Ren RT, Yi F, Suzuki K, et al. Direct reprogramming of porcine fibroblasts to neural progenitor cells. Protein Cell. 2014;5(1):4-7. doi: 10.1007/s13238-013-0015-y.
28. Lee JH, Mitchell RR, McNicol JD, Shapovalova Z, Laronde S, Tanasijevic B, et al. Single transcription factor conversion of human blood fate to NPCs with CNS and PNS developmental capacity. Cell Rep. 2015;11(9):1367-76. doi: 10.1016/j.celrep.2015.04.056.
29. Shahbazi E, Moradi S, Nemati S, Satarian L, Basiri M, Gourabi H, et al. Conversion of Human Fibroblasts to Stably Self-Renewing Neural Stem Cells with a Single Zinc-Finger Transcription Factor. Stem Cell Reports. 2016;6(4):539-51. doi: 10.1016/j.stemcr.2016.02.013.
30. Yuan Y, Tang X, Bai YF, Wang S, An J, Wu Y, et al. Dopaminergic precursors differentiated from human blood-derived induced neural stem cells improve symptoms of a mouse Parkinson's disease model. Theranostics. 2018;8(17):4679-94. doi: 10.7150/thno.26643.
31. Nakanishi M, Otsu M. Development of Sendai virus vectors and their potential applications in gene therapy and regenerative medicine. Curr Gene Ther. 2012;12(5):410-6. doi: 10.2174/156652312802762518.
32. Fusaki N, Ban H, Nishiyama A, Saeki K, Hasegawa M. Efficient induction of transgene-free human pluripotent stem cells using a vector based on Sendai virus, an RNA virus that does not integrate into the host genome. Proc Jpn Acad Ser B Phys Biol Sci. 2009;85(8):348-62. doi: 10.2183/pjab.85.348.

33. Seki T, Yuasa S, Oda M, Egashira T, Yae K, Kusumoto D, et al. Generation of induced pluripotent stem cells from human terminally differentiated circulating T cells. Cell Stem Cell. 2010;7(1):11-4. doi: 10.1016/j.stem.2010.06.003.
34. Ban H, Nishishita N, Fusaki N, Tabata T, Saeki K, Shikamura M, et al. Efficient generation of transgene-free human induced pluripotent stem cells (iPSCs) by temperature-sensitive Sendai virus vectors. Proc Natl Acad Sci U S A. 2011;108(34):14234-9. doi: 10.1073/pnas.1103509108.
35. Tongkobpetch S, Rungsiwiwut R, Pruksananonda K, Suphapeetiporn K, Shotelersuk V. Generation of two human iPSC lines (MDCUi001-A and MDCUi001-B) from dermal fibroblasts of a Thai patient with X-linked osteogenesis imperfecta using integration-free Sendai virus. Stem Cell Res. 2019;39:101493.doi: 10.1016/j.scr.2019.101493.
36. Khan M, Gasser S. Generating Primary Fibroblast Cultures from Mouse Ear and Tail Tissues. J Vis Exp. 2016(107). doi: 10.3791/53565.
37. Sajad M, Zargan J, Zargar MA, Sharma J, Umar S, Arora R, et al. Quercetin prevents protein nitration and glycolytic block of proliferation in hydrogen peroxide insulted cultured neuronal precursor cells (NPCs): Implications on CNS regeneration. Neurotoxicology. 2013;36:24-33. doi: 10.1016/j.neuro.2013.01.008.
38. Phakdeedindan P, Setthawong P, Tiptanavattana N, Rungarunlert S, Ingrungruanglert P, Israsena N, et al. Rabbit induced pluripotent stem cells retain capability of in vitro cardiac differentiation. Exp Anim. 2019;68(1):35-47. doi: 10.1538/expanim.18-0074.
39. Wang L, Wang L, Huang W, Su H, Xue Y, Su Z, et al. Generation of integration-free neural progenitor cells from cells in human urine. Nat Methods. 2013;10(1):84-9. doi: 10.1038/nmeth.2283.
40. Tang X, Wang S, Bai Y, Wu J, Fu L, Li M, et al. Conversion of adult human peripheral blood mononuclear cells into induced neural stem cell by using episomal vectors. Stem Cell Res. 2016;16(2):236-42. doi: 10.1016/j.scr.2016.01.016.
41. Kim SM, Kim JW, Kwak TH, Park SW, Kim KP, Park H, et al. Generation of Integration-free Induced Neural Stem Cells from Mouse Fibroblasts. J Biol Chem. 2016;291(27):14199-212. doi: 10.1074/jbc.M115.713578.

42. Lee M, Ha J, Son YS, Ahn H, Jung KB, Son MY, et al. Efficient exogenous DNA-free reprogramming with suicide gene vectors. Exp Mol Med. 2019;51(7):1-12. doi: 10.1038/s12276-019-0282-7.
43. Meyer S, Wörsdörfer P, Günther K, Thier M and Edenhofer F. Derivation of adult human fibroblasts and their direct conversion into expandable neural progenitor cells. J Vis Exp. 2015; (101): e52831. doi: 10.3791/52831
44. Thier MC, Hommerding O, Panten J, Pinna R, Garcia-Gonzalez D, et al. Identification of embryonic neural plate border stem cells and their generation by direct reprogramming from adult human blood cells. Cell Stem Cell. 2019;24: 1–17.
45. Thier M, Wörsdörfer P, Lakes YB, Gorris R, Herms S, et al. Direct conversion of fibroblasts into stably expandable neural stem cells. Cell Stem Cell. 2012; 10: 473–479.
46. Bai R, Chang Y, Saleem A, Wu F, Tian L, et al. Ascorbic acid can promote the generation and expansion of neuroepithelial-like stem cells derived from hiPS/ES cells under chemically defined conditions through promoting collagen synthesis. Stem Cell Res Ther. 2021;12(1):48. doi: 10.1186/s13287-020-02115-6.PMID: 33422132 Free PMC article.

9. Acknowledgements

We would like to express our gratitude to the following experts and institutions for their contributions: Thanks to Prof. Dr. Kamthorn Pruksananonda and Pranee Numchaisrika from the Department of Obstetrics and Gynecology, Faculty of Medicine, Chulalongkorn University, for the equipment provision and technical assistance. Additionally, we would like to thank Sirikron Pamonsupornvichit for doing the G-banding karyotype and Wipawee Pavarajarn for assisting with the cell reprogramming process. Furthermore, we would like to thank Supath Tantivitayamas and Onvara Ritudomphol from Histocenter Thailand Co., Ltd. for providing a Leica DMi8 inverted fluorescent microscope equipped with a Leica DFC7000 camera, Utarat imsaard from Hollywood International Ltd. for providing a DS-Ri2 camera and the LUCIA Cytogenetics System, and

Nawapol Udpuay and staff of Mahidol University-Frontier Research Facility (MU-FRF), Mahidol University for providing the flow cytometry machine and Jess automated western blotting. Finally, we would like to express our deepest gratitude to the Monitoring and Surveillance Center for Zoonotic Diseases in Wildlife and Exotic Animals, Mahidol University, and their staff for providing laboratory space and technical help.

10. Funding

This research project is funded by the Program Management Unit for Human Resources & Institutional Development, Research and Innovation [Grant number: B05F630046] and Mahidol University [Basic Research Fund: fiscal year 2021].

11. Author information

11.1 Affiliations

Laboratory of Cellular Biomedicine and Veterinary Medicine, Faculty of Veterinary Science, Mahidol University, Nakhon Pathom 73170, Thailand

Warunya Chakritbudsabong, Phakhin Juntahirun, Sasitorn Rungarunlert

Department of Preclinic and Applied Animal Science, Faculty of Veterinary Science, Mahidol University, Nakhon Pathom 73170, Thailand

Warunya Chakritbudsabong, Phakhin Juntahirun, Sasitorn Rungarunlert

Department of Anatomy, Faculty of Medicine, Srinakharinwirot University, Bangkok, Thailand

Ruttachuk Rungsiwiwut

The Monitoring and Surveillance Center for Zoonotic Disease in Wildlife and Exotic Animals (MOZWE), Faculty of Veterinary Science, Mahidol University, Nakhon Pathom 73170, Thailand

Ladawan Sariya, Nattarun Chaisilp, Somjit Chaiwattanarungruengpaisan

11.2 Contributions

Each author contributed the following: WC and SR were responsible for funding acquisition, conceptualization, the original draft manuscript writing, and execution of the majority of experiments, including the establishment and characterization of piNSCs. RR was responsible for the initial cell reprogramming process. LS was responsible for the molecular analysis. PJ, NC, and SC conducted cell culture, immunofluorescence and imaging analyses. WC analyzed the data. JF, RR, and SR all contributed to the review and editing of the final manuscript. All authors approved the final version submitted for publication.

11.3 Corresponding authors

Correspondence to Sasitorn Rungarunlert

12. Ethics declarations

12.1 Ethics approval and consent to participate

Ethical approval for the use of animals in this study was granted by the Institutional Animal Care and Use Committee at Faculty of Veterinary Science, Mahidol University, Thailand (Approval ID: MUVS-2015-49). The Mahidol University Biosafety Subcommittee approved the use of all

biohazardous materials in this study, including animal cells and recombinant DNA (MU-2013-002).

12.2 Consent for publication

Not applicable

12.3 Competing interests

The authors state that no commercial or financial connections that might be regarded as a possible conflict of interest existed during the conduct of the research.

13. Figure captions

Figure 1. Direct Reprogramming of PTFs into Transgene-Free piNSC lines using the Sendai virus. (A) Schematic diagram illustrating the timeframe of the piNSC generation. **(B)** Phase-contrast image of PTFs after overnight treatment with the Sendai virus transfection. **(C)** Phase-contrast image of the piNSC-like emerging colony at 21 days after transfection (P0). **(D)** High-magnification image of cells in the inset in (C). **(E)** Phase-contrast image of piNSC- like colonies after first passage (P1), which are positive for the early NSC markers PAX6/NESTIN (**F**, red/green) and SOX2 (**G**, red). DAPI staining is blue. These colonies can be propagated further to produce self-renewing iNSCs that are stably self-renewing. Morphology of iNSCs at P5 when cultured in a Matrigel-coated dish **(H)** and formed neurospheres when maintained in suspension culture **(I)**. piNSC-derived neurons showed typical neuronal morphology **(J).** Scale bars represent 50 μm in (**B**), (**D**)–(**H**), 100 μm in (**I**), and 20 μm in (**J**).

Figure 2. Characterization of Transgene-Free piNSC lines. (A) piNSCs can be maintained indefinitely after more than 40 passages. piNSCs was detected neural stem cell markers (PAX6, SOX2 and NESTIN), pluripotency marker (OCT4) and cell proliferation marker (KI67) using fluorescence microscopy. **(B)** Quantitative analysis of the neural stem cell markers and cell proliferation marker in the piNSC lines. Means with different lowercase letters are significantly different at $P < 0.05$. **(C)** Western blot images of neural stem cells markers (PAX6 and SOX2) expression and quantification of the western blot results. β-Actin was used as an internal control. Means with different lowercase letters are significantly different at $P < 0.05$. **(D)** G-band analysis of the piNSCs showed a normal karyotype. Scale bars represent 10 μm in (**A**) Morphology (P20), and 50 μm in (**A**) immunofluorescent images.

Figure 3. Neurosphere formation of piNSC lines. (A) Phase-contrast image of neurospheres on day 7. **(B)** Average of area of neurospheres. Means with different lowercase letters are significantly different at $P < 0.05$. **(C)** Immunofluorescent staining of neurospheres exhibits the expression of neural stem cell markers (PAX6 and SOX2) and cell proliferation marker. Scale bars represent 100 μm in (**A**) and (**C**)

Figure 4. *In Vitro* Differentiation Potential of piNSC lines. (A) Phase-contrast image of neurons derived from both piNSC lines after day 7 and day 14 of differentiation. **(B)** Neurons differentiated from both piNSC lines expressed immature neuronal marker (TUJ1), mature neuronal marker (MAP2), synaptic protein synaptophysin (SYP), dopamine-secreting neurons (TH) and astrocyte (GFAP). **(C)** Quantitative analysis of the neurons and astrocytes derived from piPSC lines. The mean fluorescence signals for TUJ1, MAP2, SYP, TH and GFAP were measured in 20 images per marker in each cell lines under identical optical settings. Means with different lowercase letters are significantly different at $P < 0.05$. **(D)** Western blot images of immature neuronal (TUJ1),

mature neuronal (MAP2) and astrocyte (GFAP) expression and quantification of the western blot results. β-Actin was used as an internal control. Means with different lowercase letters are significantly different at $P < 0.05$. Scale bars represent 20 μm in **(A)**, and 50 μm in **(B)**.

Figure 5. The effect of ascorbic acid on cryopreservation of piNSCs. (A) Cell proliferation was determined with KI67, and cell apoptosis was determined using CASPASE3 at different ascorbic acid concentrations 24 hours after thawing. (B) the ratio of KI67-positive cells at varied ascorbic acid concentrations 24 hours after thawing. (C) The proliferation of cells was determined using the CCK-8 test at varied ascorbic acid concentrations and periods following freezing. (D) The Griess reagent was used to determine the nitrite level at varied ascorbic acid concentrations 24 hours after thawing. Scale bars represent 50 μm in (A).

Figures

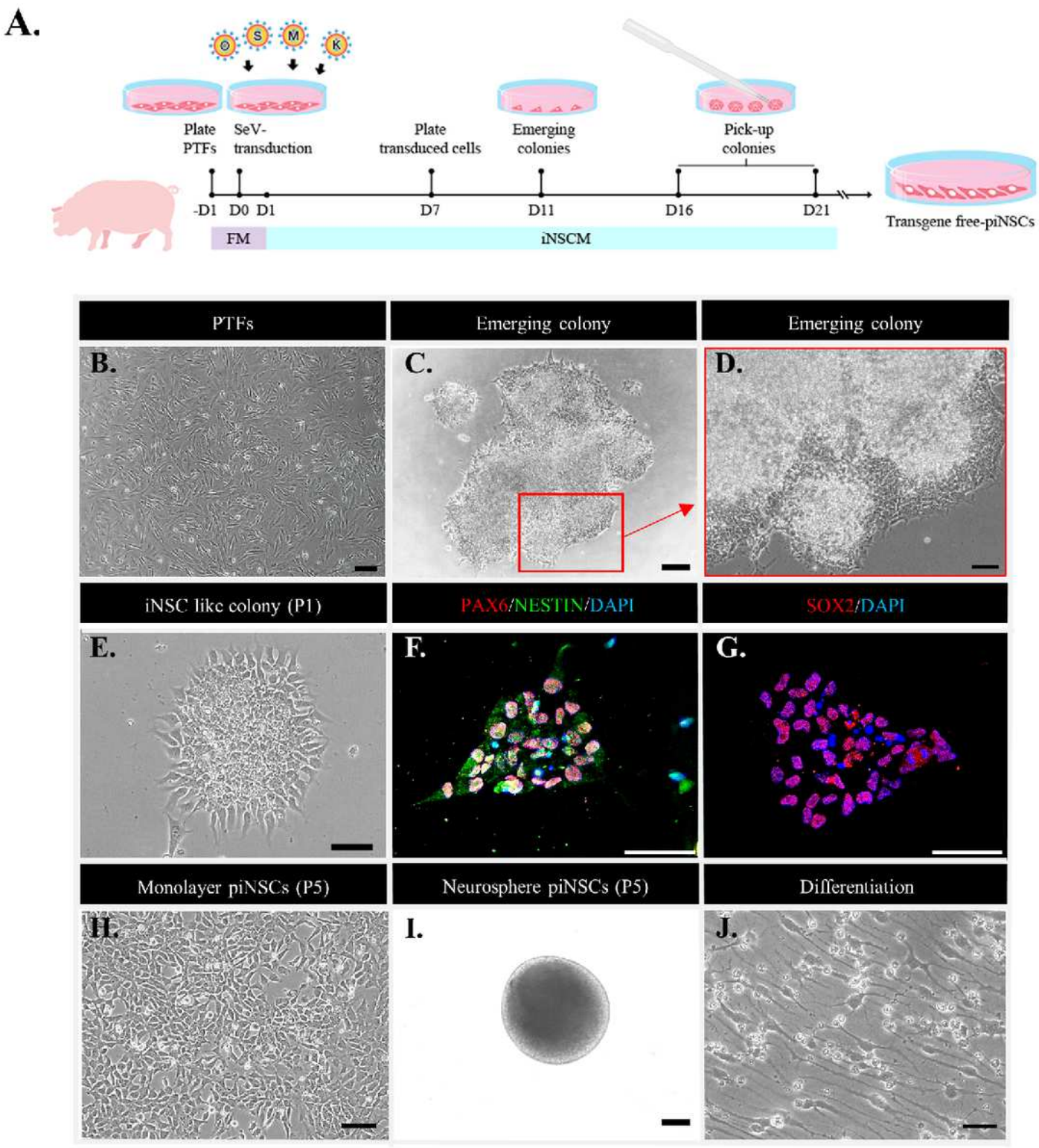

Figure 1

Direct Reprogramming of PTFs into Transgene-Free piNSC lines using the Sendai virus. (A) Schematic diagram illustrating the timeframe of the piNSC generation. (B) Phase-contrast image of PTFs after overnight treatment with the Sendai virus transfection. (C) Phase-contrast image of the piNSC-like

emerging colony at 21 days after transfection (P0). (D) High-magnification image of cells in the inset in (C). (E) Phase-contrast image of piNSC- like colonies after first passage (P1), which are positive for the early NSC markers PAX6/NESTIN (F, red/green) and SOX2 (G, red). DAPI staining is blue. These colonies can be propagated further to produce self-renewing iNSCs that are stably self-renewing. Morphology of iNSCs at P5 when cultured in a Matrigel-coated dish (H) and formed neurospheres when maintained in suspension culture (I). piNSC-derived neurons showed typical neuronal morphology (J). Scale bars represent 50 μm in (B), (D)−(H), 100 μm in (I), and 20 μm in (J).

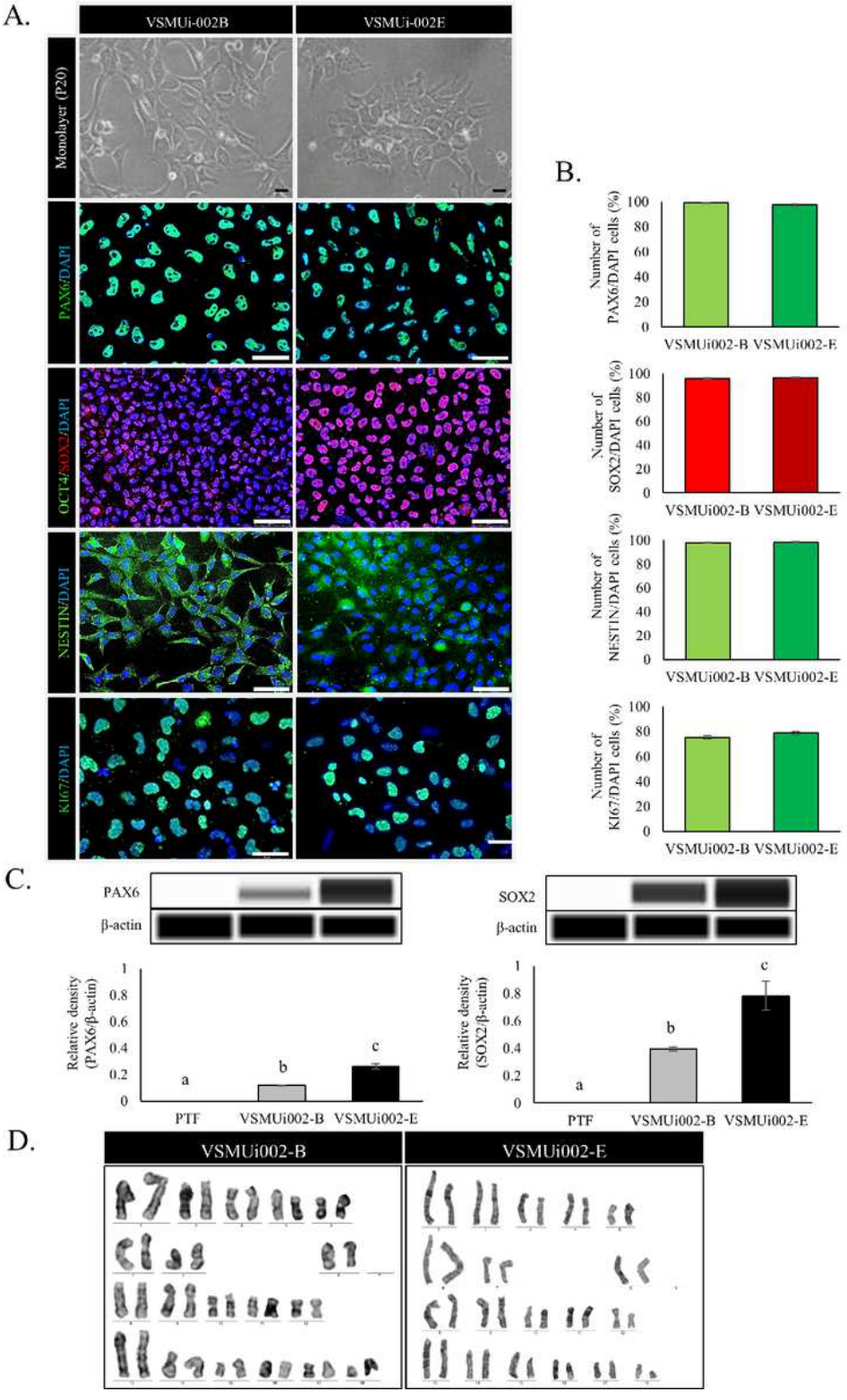

Figure 2

Characterization of Transgene-Free piNSC lines. (A) piNSCs can be maintained indefinitely after more than 40 passages. piNSCs was detected neural stem cell markers (PAX6, SOX2 and NESTIN), pluripotency marker (OCT4) and cell proliferation marker (KI67) using fluorescence microscopy. (B) Quantitative analysis of the neural stem cell markers and cell proliferation marker in the piNSC lines. Means with different lowercase letters are significantly different at $P < 0.05$. (C) Western blot images of neural stem cells markers (PAX6 and SOX2) expression and quantification of the western blot results. β-Actin was used as an internal control. Means with different lowercase letters are significantly different at $P < 0.05$. (D) G-band analysis of the piNSCs showed a normal karyotype. Scale bars represent 10 μm in (A) Morphology (P20), and 50 μm in (A) immunofluorescent images.

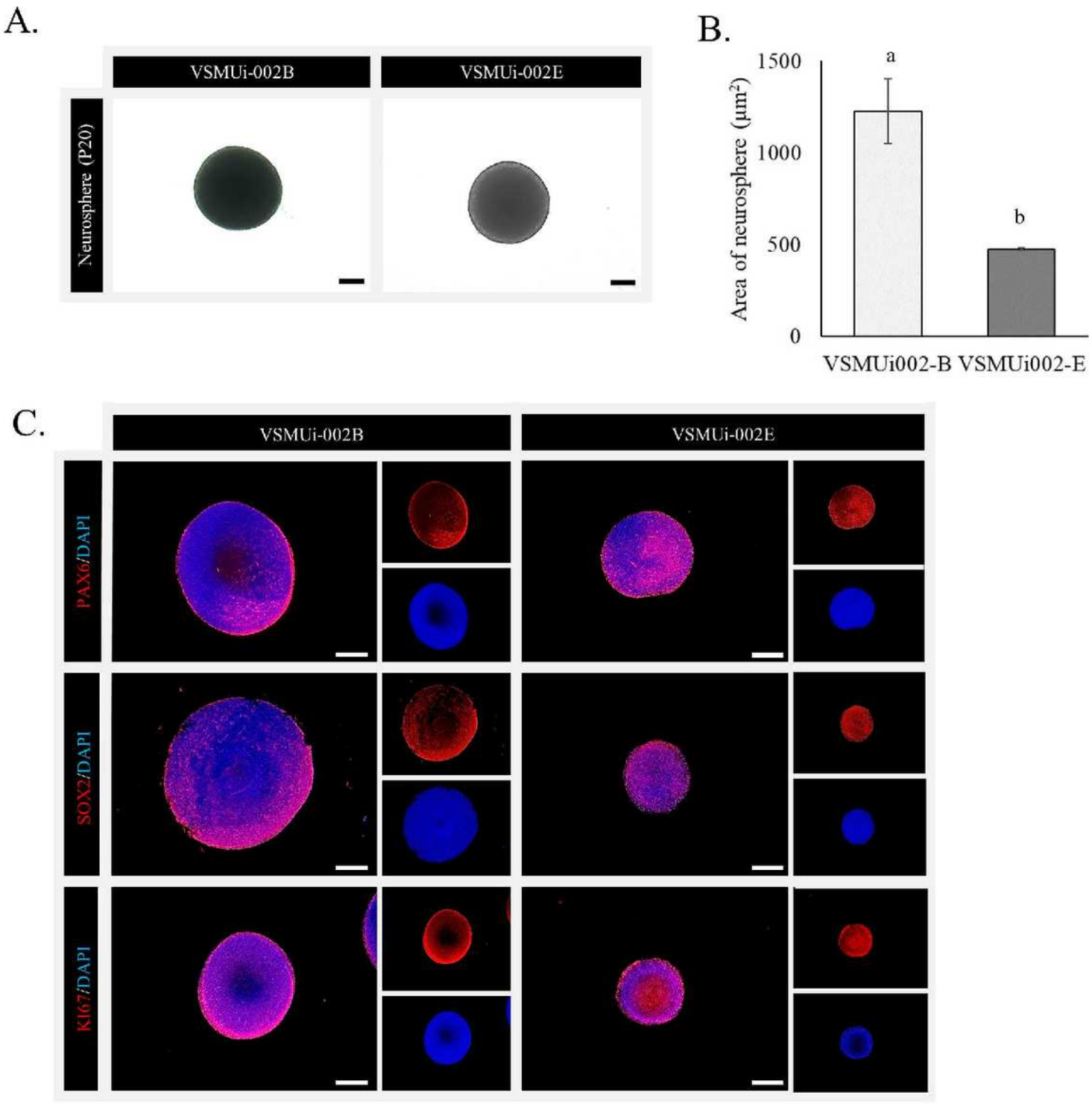

Figure 3

Neurosphere formation of piNSC lines. (A) Phase-contrast image of neurospheres on day 7. (B) Average of area of neurospheres. Means with different lowercase letters are significantly different at $P < 0.05$. (C) Immunofluorescent staining of neurospheres exhibits the expression of neural stem cell markers (PAX6 and SOX2) and cell proliferation marker. Scale bars represent 100 μm in (A) and (C)

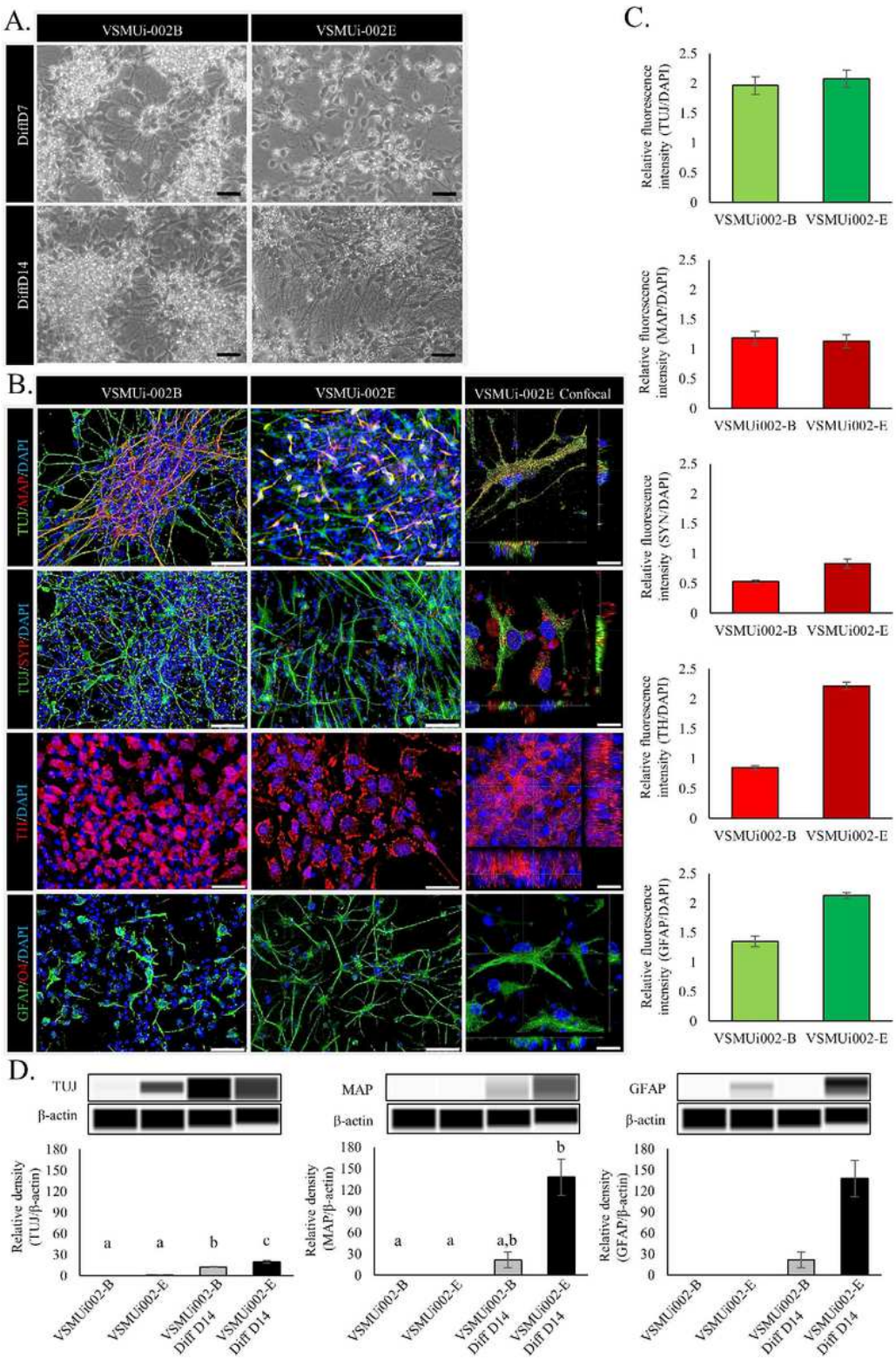

Figure 4

In Vitro Differentiation Potential of piNSC lines. (A) Phase-contrast image of neurons derived from both piNSC lines after day 7 and day 14 of differentiation. (B) Neurons differentiated from both piNSC lines expressed immature neuronal marker (TUJ1), mature neuronal marker (MAP2), synaptic protein synaptophysin (SYP), dopamine-secreting neurons (TH) and astrocyte (GFAP). (C) Quantitative analysis of the neurons and astrocytes derived from piPSC lines. The mean fluorescence signals for TUJ1, MAP2,

SYP, TH and GFAP were measured in 20 images per marker in each cell lines under identical optical settings. Means with different lowercase letters are significantly different at P < 0.05. (D) Western blot images of immature neuronal (TUJ1), mature neuronal (MAP2) and astrocyte (GFAP) expression and quantification of the western blot results. β-Actin was used as an internal control. Means with different lowercase letters are significantly different at P < 0.05. Scale bars represent 20 μm in (A), and 50 μm in (B).

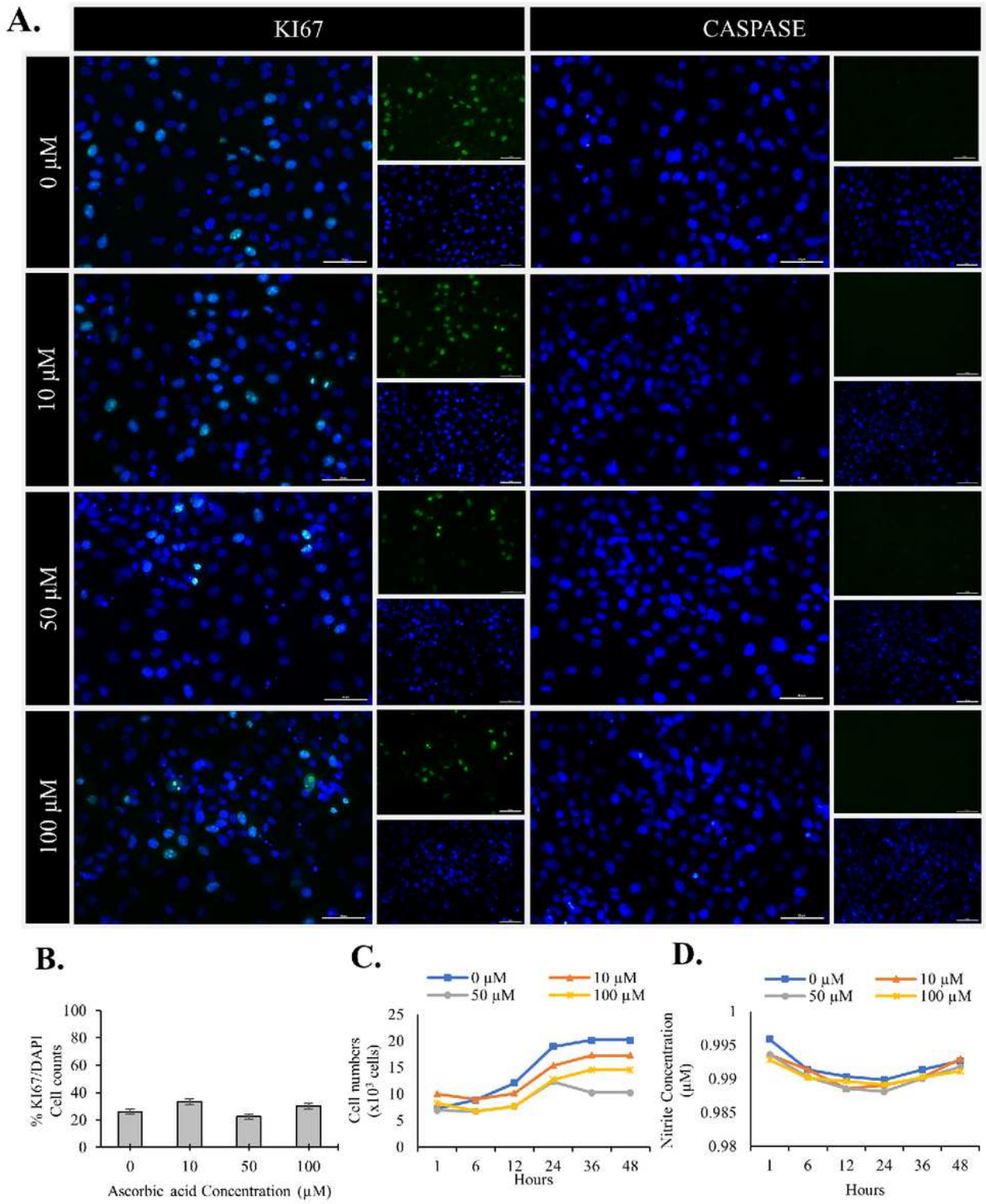

Figure 5

The effect of ascorbic acid on cryopreservation of piNSCs. (A) Cell proliferation was determined with KI67, and cell apoptosis was determined using CASPASE3 at different ascorbic acid concentrations 24 hours after thawing. (B) the ratio of KI67-positive cells at varied ascorbic acid concentrations 24 hours after thawing. (C) The proliferation of cells was determined using the CCK-8 test at varied ascorbic acid concentrations and periods following freezing. (D) The Griess reagent was used to determine the nitrite level at varied ascorbic acid concentrations 24 hours after thawing. Scale bars represent 50 μm in (A).

Supplementary Files

This is a list of supplementary files associated with this preprint. Click to download.

- Table1Antibodiesusedforimmunofluorescence.pdf